Capacitive coupling synchronizes autonomous microfluidic oscillators

Sasha Cai Lesher-Perez[1,2,3,Φ], Chao Zhang[1,2,4,5Φ], Shuichi Takayama[1,2,6,7*]

[1] Department of Biomedical Engineering, University of Michigan, Ann Arbor, MI 48109, USA

[2] Biointerfaces Institute, 2800 Plymouth Road, Ann Arbor, MI 48109, USA

[3] Chemical and Biomolecular Engineering, University of California, Los Angeles, CA 90095, USA

[4] Key Laboratory of Low-Grade Energy Utilization Technologies and Systems, Chongqing University, Chongqing 400030, China

[5] Institute of Engineering Thermophysics, Chongqing University, Chongqing 400030, China

[6] The Parker H. Petit Institute of Bioengineering and Bioscience, Georgia Institute of Technology, 315 Ferst Dr NW, Atlanta, GA 30332, USA

[7] Wallace H. Coulter Department of Biomedical Engineering, Georgia Institute of Technology and Emory School of Medicine, Atlanta, GA 30332, USA

[Φ] These authors contributed equally to this work.

* Author to whom correspondence should be addressed:

Professor Shuichi Takayama, 4018 Engineered Biosystems Building, 950 Atlantic Dr NW, Atlanta, GA 30332, USA

E-Mail: takayama@gatech.edu; Tel.: +1-404-385-5722;

ABSTRACT

Even identically-designed autonomous microfluidic oscillators have device-to-device oscillation variability that arises due to inconsistencies in fabrication, materials, and operation conditions. This work demonstrates, experimentally and theoretically, that with appropriate capacitive coupling these microfluidic oscillators can be synchronized. The size and characteristics of the capacitive coupling needed and the range of input flow rate differences that can be synchronized are also characterized. In addition to device-to-device variability, there is also within-device oscillation noise that arises. An additional advantage of coupling multiple fluidic oscillators together is that the oscillation noise decreases. The ability to synchronize multiple autonomous oscillators is also a first step towards enhancing their

usefulness as tools for biochemical research applications where multiplicate experiments with identical temporal-stimulation conditions are required.

INTRODUCTION

Efforts to minimize requirements for external controllers has led to the development of self-switching microfluidic circuits [1–5]. An autonomous fluid circuit type that is of general usefulness in biology are microfluidic oscillators that convert two constant input flows into alternating fluid flows to allow periodic delivery of chemicals or to mimic the pulsatile nature of biological fluid flows such as blood flow [1,6]. A key requirement for biological studies is the ability to perform multiplicate experiments and controls. This can be a challenge for self-switching fluidic circuits because of circuit-to-circuit variability that leads to slightly different oscillation characteristics. This paper describes a strategy to overcome this challenge using capacitive coupling to synchronize multiple oscillators. We also demonstrate that coupled oscillator systems have an additional advantage of reduced noise. That is, intra-device variations in oscillation frequency and amplitude of each oscillator is reduced when multiple oscillators are coupled together.

First described by Huygens, in the classical case of periodic self-sustained oscillators [7], interactions or coupling between the individual systems can lead to synchronized behaviors [8] depending on the coupling strength [9]. More specifically, weak coupling results in frequency pulling of one oscillator towards the other but with incomplete synchronization particularly with larger phase shifts and frequency mismatch. A stronger coupling will lead to full synchronization. An overly strong coupling of out of phase oscillators effectively quenches each other, pulling each oscillator unit into a zero-amplitude standstill or "oscillation death" [10]. While these general properties of coupled oscillators are well known, it is not clear if appropriate coupling can be realized for self-switching microfluidic oscillator systems. Here, we performed physical experiments along with simulations of coupling two or four fluidic oscillators through capacitive units. As anticipated, we found that the minimum coupling strength required for synchronization is dependent on the period difference between coupled fluidic oscillators. Experimentally, synchronization was demonstrated between fluidic oscillators with period differences as great as 61 seconds. We additionally show through simulations that there is a unique minimum coupling capacitance requirement, even between fluidic oscillators with relatively small differences in oscillation periods, and that this is dictated by the parasitic capacitance of the fluidic oscillator's switching valves. While this work focused on the synchronization of coupled oscillators, simulations were used to predict conditions where disruption of the oscillators could occur. Oscillator disruption included states in which an oscillator would "leak" and have signal from each input being simultaneously output even if oscillating between various states, or amplitude death where the output signal stopped oscillating and remained at an amplitude standstill. Simulations predicted a narrow range of conditions where oscillation disruption and amplitude death should occur. We were unable to create such conditions in our experimental system. We suspect that this discrepancy arises from the variation inherent in experimental systems whereas simulations were performed with very discrete conditions.

Even for a single oscillator circuit, real-life oscillations are "noisy" where frequency and phase fluctuations caused by inherent instability of syringe pumps as well as leaks, debris, and other potential fabrication variations. Generally, a well-known incidental benefit of coupled oscillators is the effect of "noise reduction" [11,12]. We show experimentally that

this also applies to coupled fluidic oscillators; resulting in more uniform and consistent operation compared to non-coupled individual oscillators. Furthermore, this noise reduction effect was more significant for a system with four coupled oscillators as compared to two coupled oscillators. These proof-of-principle demonstrations and description of the mechanisms of operation and beneficial characteristics of coupled fluidic oscillators not only advance the field of microfluidics but are envisioned to facilitate transfer of such technology from microfluidic device developers to biological end users [13].

MATERIALS AND METHODS

Device Fabrication

Methods used for microfluidic oscillators and coupling capacitor master mold fabrication were similar to those previously presented [14]. The microfluidic oscillator device consists of three polydimethylsiloxane (PDMS) layers assembled as previously described. Briefly, the device features (66 μm or 100 μm height, for oscillators and coupling capacitor, respectively) were imprinted in the top and bottom layers, and a PDMS membrane (target thickness: 11 μm) was positioned between them. 1:10 PDMS (Sylgard 184, Dow Corning, Midland, MI, USA) was poured onto the master mold and allowed to cure within a gravity convection oven at 60 °C for 6 h. The cured PDMS slab was then removed from the mold and cut into individual device layers. Concurrently, PDMS membranes were fabricated by spin-coating 1:10 PDMS onto glass slides pre-treated with silane. PDMS membranes were then cured within a gravity convection oven for 5 min at 120 °C and 10 min at 60 °C. Prior to final assembly, a 2-mm biopsy punch was used to remove PDMS from the inlet and outlet ports of the top device layer. The bottom layer and membrane were then treated by plasma oxidation (Covance MP, FemtoScience, Hwaseong-si, Gyeonggi-do, South Korea) to facilitate bonding and, following bonding, were then placed in a gravity convection oven at 120 °C for 5 min and at 60 °C for 10 min. Thru-holes were then made in the membrane to allow fluid communication between the top and bottom device layers, using a 350-μm biopsy punch (Ted Pella Inc., Redding, CA, USA). The top layer was then treated by plasma oxidation to facilitate bonding with the membrane-bottom layer assembly. Following treatment, but preceding bonding, the normally closed region of the top layer was "deactivated" by being brought into direct contact with an unoxidized PDMS "stamp". Following final bonding, assembled devices were incubated for 2 min within a gravity convection oven at 120 °C. Coupling capacitors were fabricated in the same fashion, except they did not require thru-holes to be punched within them, or have any region deactivated.

Coupling simulations

In the present study, commercial software (PLECS, Plexim GmbH, Switzerland) was used for the numerical simulation of the microfluidic oscillators and coupling capacitor. Based on electro-hydraulic circuit analogy, microfluidic channels are simulated as electric resistors, flexible membranes correspond to capacitors, and the flow rates are transformed into electric current. The input flow rates and coupling capacitance were adjusted according to the settings

of each experiment. All other parameters used in the model were from experimental measurements [15]. A schematic of the model is shown in Fig. SI 1a.

Microfluidic Oscillator Testing and Data Processing

A syringe pump (Model KDS220, KD Scientific, Holliston, MA, USA) was used to provide constant volumetric flow to the device. 3 mL syringes (Becton, Dickinson and Company, Franklin Lakes, NJ, USA), filled with filtered deionized water mixed with and without food coloring, were connected to the inlet ports via Tygon tubing (Saint-Gobain™ Tygon™ R-3603 Clear Laboratory Tubing, Saint-Gobain Performance Plastics, Akron, OH, USA). Microfluidic oscillators were monitored by using a 3-way valve to connect pressure sensors (Model 142PC05D, Honeywell, NJ, USA) at the device inlets via Tygon tubing (R-3603 Clear Laboratory Tubing) to measure source pressure. Source pressure data was collected for valves to quantify pressure buildup and release corresponding to fluid accumulation and evacuation, respectively, through the valves. The occurrence of fluidic oscillations and the coincident timing of these oscillations relative to source pressure profiles were initially verified visually, all subsequent quantification and assessment, however, was performed using source pressure data. Data was obtained at a sampling rate of 1000 Hz, every 100 data points were averaged (resulting in 1 data point per 100 ms), and stored using LabVIEW (National Instruments, Austin, TX, USA). Voltage data were collected using LabVIEW and processed to demonstrate oscillation frequency of the microfluidic oscillators tested.

RESULTS AND DISCUSSIONS

Two separate microfluidic oscillators, designed and fabricated with the same parameters when operated under the same infusion flow rate, e.g. 5 µL/min (Fig. 1a), are expected to execute equivalent operations. Yet, like any manufacturing process, inherent variability exists. Additional idiosyncrasies [14] arise due to the instabilities of syringe pump systems [16] and syringes [17]. Real-life imperfections such as minor leaks and introduction of debris or particulates into the circuits can also cause inconsistencies. Combined, these parameters lead to device-to-device variability as shown experimentally for two presumably "identical" oscillators operated under "identical" conditions as visualized in a pressure change over time plot (Fig. 1b) and a phase portrait (Fig. 1c). The phase portrait is a geometric representation of the trajectories of these two dynamical systems, demonstrating the pressure trajectories of the mirrored valves in each oscillator, indicating the interaction between the two oscillators. Increased synchronization is typically denoted by a consistently repeated pattern, with optimal synchronization being a linear relationship between the mirrored oscillator valves' pressure response, i.e. Fig. 2D.

In this work, we define microfluidic oscillator synchronization as the simultaneous switching by the valve units in each oscillator; where the opening and closing of the membrane valve is determined by the relative difference between the source minus gate pressure versus the threshold pressure [15]. Learning from electrical systems, we utilized various size microfluidic capacitors [18], comprised of a flexible membrane that allows exchange of fluidic energy or pressure, while keeping the actual fluids separate (Fig. SI 3a,b), to couple

the two oscillators (a schematic is shown in Fig. 1d and an actual setup can be found in Fig. SI 2). With the incorporation of the microfluidic coupling capacitor we accomplished synchronized behavior with regards to pressure profiles between the two oscillators (Fig. 1c and f).

As the size of the coupling capacitor increased, we found increased synchronization between the two coupled microfluidic oscillators (Fig. 2b, c). The measured oscillator valve pressures were implemented in eq. 1 to quantify the coupling strength afforded by different coupling capacitors.

$$\frac{d\varphi}{dt} = \Delta\omega + \varepsilon \sin\varphi, \tag{1}$$

Here ω is the natural frequency of the oscillator and $\Delta\omega$ is the frequency mismatch between the oscillators, ε is the coupling strength, and φ is phase difference of the two oscillators; for brief description and derivation of equation (1) for the analysis of phase synchronization see supplemental information, or for more in depth description see previous literature on oscillator locking and synchronization [19,20]. Using the empirical data, we determine the maximum coupling strength achieved by each coupling capacitor used within our system.

In addition to experimental studies, we performed simulations evaluating two non-coupled and coupled oscillators. We have previously shown that electrical circuit simulation software can effectively capture features of microfluidic oscillators [6,21]. Here we simulate device-to-device variability as devices with differences in the phase of oscillation or with both differences in phase and period. Simulations predicted that out of phase oscillations could be synchronized with a critical coupling capacitance of 1×10^{-14} N s/m^5 (Fig. 3) but that oscillators that are both out of phase and with different periods from each other require a stronger coupling (e.g. 1×10^{-12} N s/m^5). Additionally, we identified a minimum critical capacitance needed for effective coupling, which was dependent on the magnitude of the parasitic capacitance of the valves within the oscillators. We also note, that increasing the size, or capacitance, of the coupling capacitors minimizes the potential of oscillation disruption and amplitude death, which appears to be a condition specific response (Table SI 1), only occurring with relatively large input flowrate differences between the two oscillators, and within a relatively small window of coupling capacitance (size); this phenomena was not observed empirically, highlighting the facile synchronization of the two oscillators, by using larger coupling capacitors.

Increasing the dimension of the square microfluidic coupling capacitors resulted in increasing synchronization between oscillators. We characterized the behavior through both the pressure profiles of the valve units in each oscillator, as well as the phase portraits of these pressures. We found that by using smaller capacitors, such as the 1.5 mm x 1.5 mm capacitor, the oscillators become unstably synchronized (Fig. 2a). The coupled oscillators appear to have some synchronicity; however, they shift in and out of this synchronized state, most likely indicating that the coupling strength of 0.0915 is insufficient to reach complete entrainment, but rather produces unstable synchronization. This is further reinforced when visualizing the

phase portrait of P_1 vs. P_2, where a triangular pattern emerges, however this coordinated behavior has instability, as the positioning of this pattern shifts through the entirety of the experimental data. Increasing the coupling capacitance, we see the stable synchronization between the oscillators (Fig. 2b, c), where the phase portrait of P_1 vs. P_2 shows a consistent triangular pattern with increasingly fixed positions with increasing coupling capacitance. The coupling strength, 8.073 and 43.15, for the larger microfluidic capacitors (2.0 mm x 2.0 mm and 3.0 mm x 3.0 mm, respectively), concomitantly increases synchronization of the oscillators. Coupling of the oscillators also appeared to result in frequency stabilization, generally demonstrating a reduction in period variation with increasing coupling strength (Fig. SI 4).

The microfluidic capacitor can couple the oscillators while preventing the liquid from passing through it, however, the presence of the elastic PDMS membrane may limit the extent of the force translated from one oscillator to the other. Implementing a direct connection may be experimentally unideal for cell based experiments, as the mixing of solutions may compromise experimental conditions when utilizing differing media compositions and biomolecule stimulants; however, we identified that this results in the strongest coupling behavior (Fig. 2d). Direct coupling of the oscillators with tubing results in the source pressure waveforms being tightly synchronized, overlapping more so than that seen with microfluidic capacitor coupling, reaching a maximum coupling strength of 45.307. Additionally, the phase portrait of P_1 vs. P_2 shows a diagonal pattern, indicating a high degree of entrainment between the two oscillators. Considering methods to circumvent direct coupling and subsequent mixing of solutions, while increasing the coupling strength of the system, we simulated the implementation of two coupling capacitors, one for each set of valves. These simulations demonstrated stronger coupling phenomena when using two coupling capacitors as compared to one in that the shift from asynchronous behavior to synchronized oscillations happen at smaller coupling capacitor sizes (Table SI 1). In addition to oscillators that have even duty cycles (50% - 50% in terms of time open for each of the two valves of an oscillator) we analyzed synchronization between oscillators operated with asymmetric input flowrates that give nonsymmetrical duty cycles [14]. Figure 4 shows experiments using oscillators with asymmetric input flow rate combinations of: 1) 5 µL/min flow rates into the coupled valve units via syringes B and D, and 2.6 µL/min into the non-coupled valve units via syringe A and C; 2) 2.6 µL/min flow rates into the coupled valve units via syringes B and D, and 5 µL/min into the non-coupled valve units via syringe A and C; 3) non-paired input flow rates, with 5 µL/min input via syringes A and D, and 2.6 µL/min input via syringes B and C. When the two asymmetric oscillators are working separately, the measured periods are 132.8 s and 186.2 s, respectively. When using combination 1 we achieved synchronization in all coupling conditions except when using the smallest microfluidic coupling capacitor, whereas the other two asymmetric input flowrate combinations only resulted in synchronized behavior when the oscillators were directly connected. The oscillation periods for synchronized asymmetric oscillators was 160.0 s for the two oscillators. These experimental results with intentionally mismatched oscillator properties are consistent with the general properties of coupled oscillators that the larger the mismatch in phase and period, the more difficult it is to achieve synchronization. This inability to couple non-synchronous variations

between valves, could be remediated by increasing the coupling capacitance, or implementing dual valve coupling as presented in Table SI 1.

In biological experiments more than two microfluidic oscillators may be required to function in parallel, under the same oscillatory behavior. For example, in the study of cellular signal pathway architecture, parallel experiments might require oscillators outputting oscillatory flow with the same frequencies, but different concentrations. Figure 5a demonstrates the ability to scale oscillator coupling from two to four oscillators. The four oscillators are coupled by three capacitors with 3.0 mm chambers. All four oscillators have a constant input flow rate of 5 µL/min. The pressure profiles of the oscillators demonstrate robust entrainment (Fig. 5c). Compared to the pressure profiles of the separated four oscillators (Fig. 5b), these results demonstrate that the coupling phenomena, can be implemented when an array of synchronized oscillators are needed, as long as the coupling strength meets the minimum requirement for the system.

Beyond the practical use of experimentally maintaining similar frequencies when oscillating solution types, these coupled microfluidic oscillators also made us reflect on how these oscillators can be used to replicate different phenomena present in coupled systems. First, we noticed at lower coupling (1.5 x 1.5 mm capacitor) that beat skipping occurs and can be seen in Figure 2, where the wave forms appear to align on most of the peaks, and yet oscillator 2 will skip one of the peaks achieved by oscillator 1, subsequently resynchronizing with oscillator 1. The period data presented in Figure SI 4 further illustrates this phenomenon. Additionally, in Figure SI 4, two instances of this occurred with the 2.5 mm x 2.5 mm capacitor. Similar inputs into each of the coupled oscillators resulted in a highly synchronized behavior with a different number of cycles occurring between each "skipped beat", furthermore this aberrant behavior returned to synchrony after only missing one "beat". Though we did not investigate the skipped beats within our system, this has been previously discussed in cell-based phase locking analysis applied to biochemical circuit architecture built on oscillatory cell signaling systems [22]. Recreating such a response in a microfluidic architecture may enable a mechanically representative system, in which analogous parameters could be defined. Furthermore, we were surprised that a coherent oscillatory activity of the two paired oscillators occurred, in which both oscillator' period was dramatically decreased. This co-dependent frequency pulling was an unexpected result, as we had initially expected the frequency of one oscillator to more closely resemble the frequency of the other, rather than stabilizing at a dramatically higher frequency for both oscillators. This coherent oscillatory response of moving from a higher period, as independent oscillators, to a reduced period between the paired oscillators, extended to coupling 4 oscillators together. Integrating a larger array of oscillators together may additionally be able to provide a model system to study the collective synchrony in large scale rhythms of populations with interacting elements [23].

CONCLUSIONS

In this work we demonstrate that multiple microfluidic oscillators can be coupled via fluidic capacitors to synchronize their oscillations. Simulations identified a relationship between the

internal capacitance of the microfluidic valve units and the coupling capacitors capacitance, such that a minimal critical capacitance needs to be used to generate sufficient coupling strength to synchronize the two oscillators. Generally, the necessary critical capacitance is at least one order of magnitude higher than the parasitic capacitance of the switching valves. Microfluidic oscillators with asymmetric inflow pairings can also be synchronized, provided the oscillators are coupled through the valves receiving the larger inflows. An incidental benefit of coupled oscillators is noise reduction. Comparing coupled oscillator systems with two and four oscillators coupled together, we also observe that the noise reduction generally decreased by 2 − 7-fold. These results demonstrate usefulness of fluidic oscillators in gaining fundamental insights into the properties of real-world coupled oscillator systems that possess oscillator-to-oscillator variability as well as within oscillator noise. The ability to synchronize multiple self-switching oscillators is also a first step towards enhancing microfluidic oscillators' usefulness as a biomedical research tool for multiplicate experiments that require identical temporal-stimulation conditions.

CONFLICT OF INTEREST

The authors declare no conflict of interest.

ACKNOWLEDGEMENTS

REFERENCES

1. Mosadegh, B., Kuo, C.-H., Tung, Y.-C., Torisawa, Y., Bersano-Begey, T., Tavana, H., and Takayama, S. (2010) Integrated elastomeric components for autonomous regulation of sequential and oscillatory flow switching in microfluidic devices. *Nat. Phys.*, **6** (6), 433–437.

2. Duncan, P.N., Nguyen, T.V., and Hui, E.E. (2013) Pneumatic oscillator circuits for timing and control of integrated microfluidics. *Proc. Natl. Acad. Sci.*, **110** (45), 18104–18109.

3. Leslie, D.C., Easley, C.J., Seker, E., Karlinsey, J.M., Utz, M., Begley, M.R., and Landers, J.P. (2009) Frequency-specific flow control in microfluidic circuits with passive elastomeric features. *Nat. Phys.*, **5** (3), 231–235.

4. Toepke, M.W., Abhyankar, V.V., and Beebe, D.J. (2007) Microfluidic logic gates and timers. *Lab. Chip*, **7** (11), 1449–1453.

5. Collino, R.R., Reilly-Shapiro, N., Foresman, B., Xu, K., Utz, M., Landers, J.P., and Begley, M.R. (2013) Flow switching in microfluidic networks using passive features and frequency tuning. *Lab. Chip*, **13** (18), 3668–3674.

6. Kim, S.-J., Yokokawa, R., Cai Lesher-Perez, S., and Takayama, S. (2015) Multiple independent autonomous hydraulic oscillators driven by a common gravity head. *Nat. Commun.*, **6**, 7301.

7. Ramirez, J.P., Olvera, L.A., Nijmeijer, H., and Alvarez, J. (2016) The sympathy of two pendulum clocks: beyond Huygens' observations. *Sci. Rep.*, **6**, srep23580.

8. Rosenblum, M.G., Pikovsky, A.S., and Kurths, J. (1996) Phase Synchronization of Chaotic Oscillators. *Phys. Rev. Lett.*, **76** (11), 1804–1807.

9. Ozden, I., Venkataramani, S., Long, M.A., Connors, B.W., and Nurmikko, A.V. (2004) Strong Coupling of Nonlinear Electronic and Biological Oscillators: Reaching the ``Amplitude Death'' Regime. *Phys. Rev. Lett.*, **93** (15), 158102.

10. Author, A.P., Rosenblum, M., Kurths, J., and Hilborn, R.C. (2002) Synchronization: A Universal Concept in Nonlinear Science. *Am. J. Phys.*, **70** (6), 655–655.

11. Chang, H.-C., Cao, X., Mishra, U.K., and York, R.A. (1997) Phase noise in coupled oscillators: theory and experiment. *IEEE Trans. Microw. Theory Tech.*, **45** (5), 604–615.

12. Zhang, M., Shah, S., Cardenas, J., and Lipson, M. (2015) Synchronization and Phase Noise Reduction in Micromechanical Oscillator Arrays Coupled through Light. *Phys. Rev. Lett.*, **115** (16), 163902.

13. Rhee, M., and Burns, M.A. (2008) Microfluidic assembly blocks. *Lab. Chip*, **8** (8), 1365–1373.

14. Lesher-Perez, S.C., Weerappuli, P., Kim, S.-J., Zhang, C., and Takayama, S. (2014) Predictable Duty Cycle Modulation through Coupled Pairing of Syringes with Microfluidic Oscillators. *Micromachines*, **5** (4), 1254–1269.

15. Kim, S.-J., Yokokawa, R., and Takayama, S. (2012) Analyzing threshold pressure limitations in microfluidic transistors for self-regulated microfluidic circuits. *Appl. Phys. Lett.*, **101** (23).

16. Li, Z., Mak, S.Y., Sauret, A., and Shum, H.C. (2014) Syringe-pump-induced fluctuation in all-aqueous microfluidic system implications for flow rate accuracy. *Lab. Chip*, **14** (4), 744–749.

17. Neff, S.B., Neff, T.A., Gerber, S., and Weiss, M.M. (2007) Flow rate, syringe size and architecture are critical to start-up performance of syringe pumps. *Eur. J. Anaesthesiol.*, **24** (7), 602–608.

18. Kim, S.-J., Yokokawa, R., and Takayama, S. (2013) Microfluidic oscillators with widely tunable periods. *Lab. Chip*, **13** (8), 1644–1648.

19. Pikovsky, A., Rosenblum, M., and Kurths, J. (2000) Phase synchronization in regular and chaotic systems. *Int. J. Bifurc. Chaos*, **10** (10), 2291–2305.

20. Adler, R. (1946) A Study of Locking Phenomena in Oscillators. *Proc. IRE*, **34** (6), 351–357.

21. Kim, S.-J., Yokokawa, R., Lesher-Perez, S.C., and Takayama, S. (2012) Constant flow-driven microfluidic oscillator for different duty cycles. *Anal. Chem.*, **84** (2), 1152–1156.

22. Jovic, A., Howell, B., Cote, M., Wade, S.M., Mehta, K., Miyawaki, A., Neubig, R.R., Linderman, J.J., and Takayama, S. (2010) Phase-Locked Signals Elucidate Circuit Architecture of an Oscillatory Pathway. *PLOS Comput. Biol.*, **6** (12), e1001040.

23. Bottani, S. (1995) Pulse-coupled relaxation oscillators: from biological synchronization to Self-Organized Criticality. *Phys. Rev. Lett.*, **74** (21), 4189–4192.
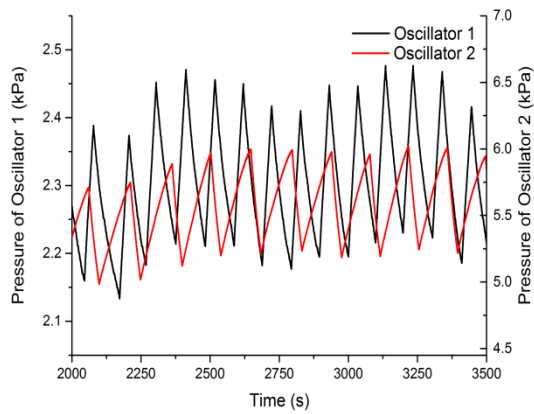
Figure 1

(a)   (d)
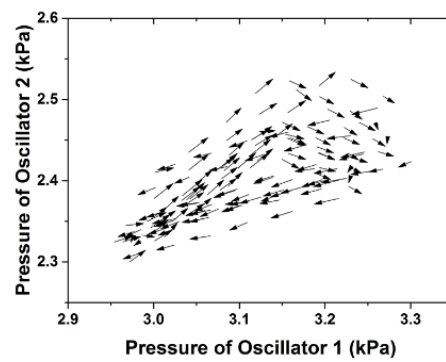
(b)   (e)

(c)   (f)
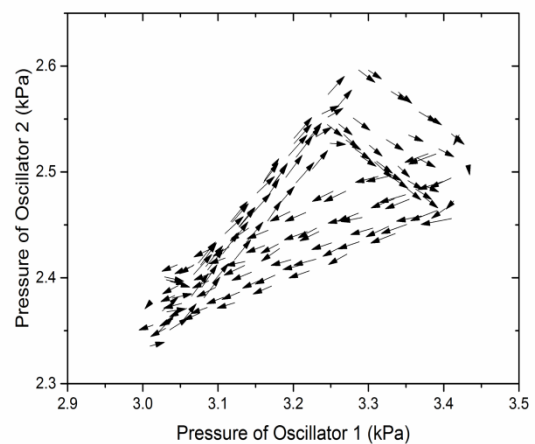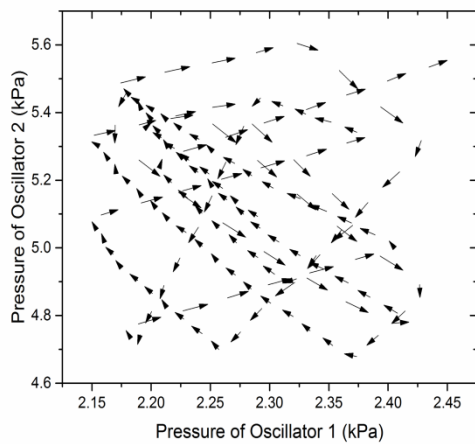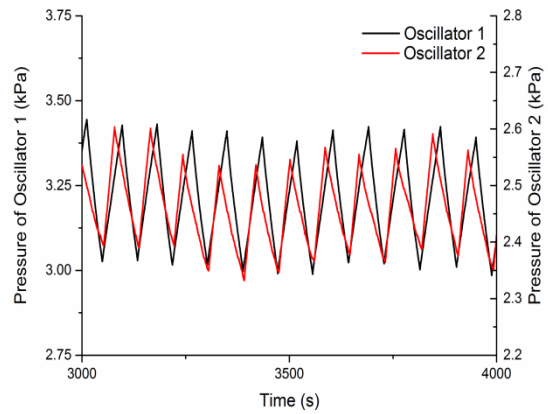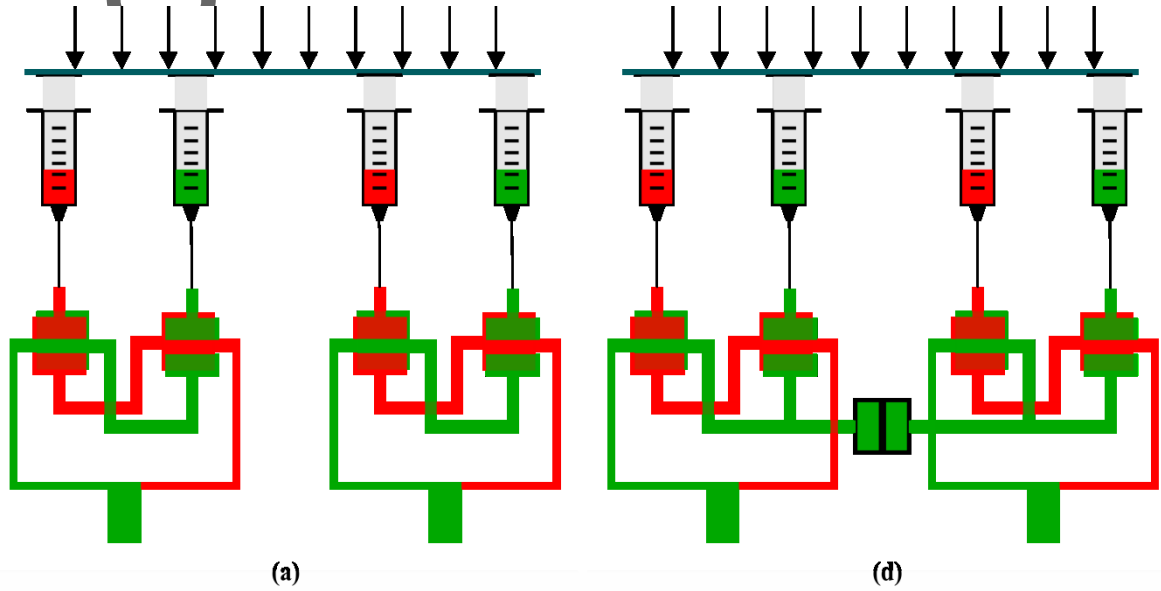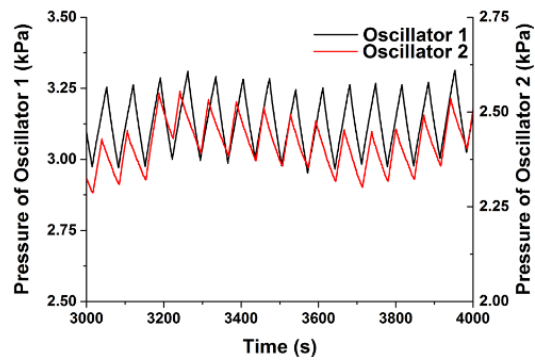
Figure 2

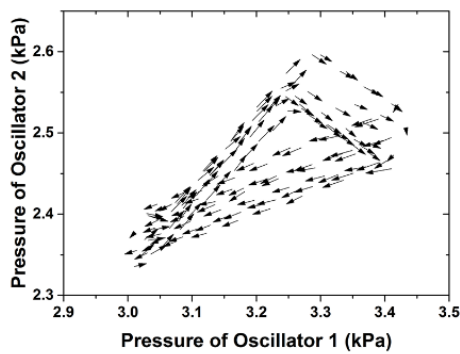Capacitor size = 1.5 mm, coupling strength ε = 0.0915   Capacitor size = 2.0 mm, coupling strength ε = 8.073
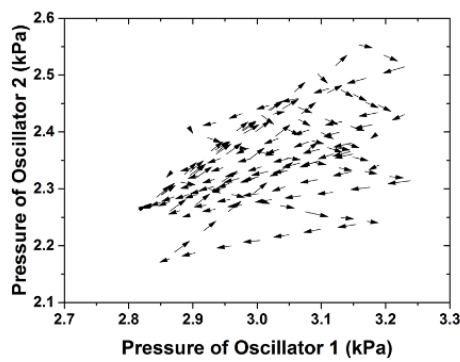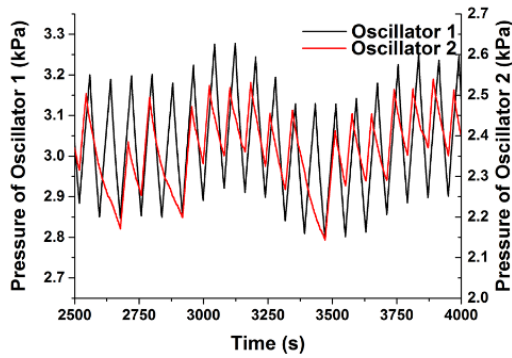
(a)   (b)

Capacitor size = 3.0 mm, coupling strength ε = 43.15   Direct connection, coupling strength ε = 45.307
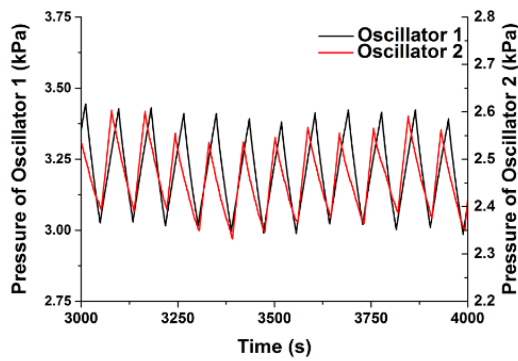
(c)   (d)

Figure 3

Figure 4

(a)

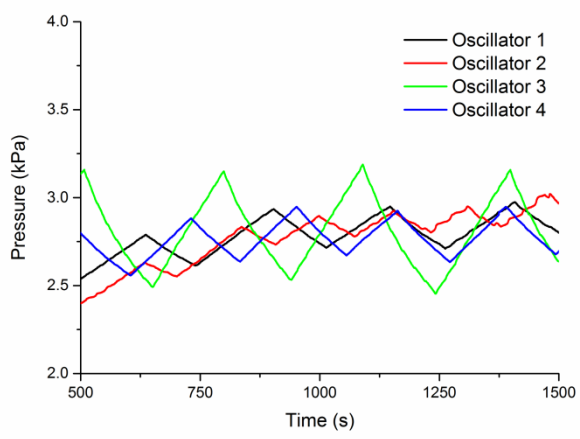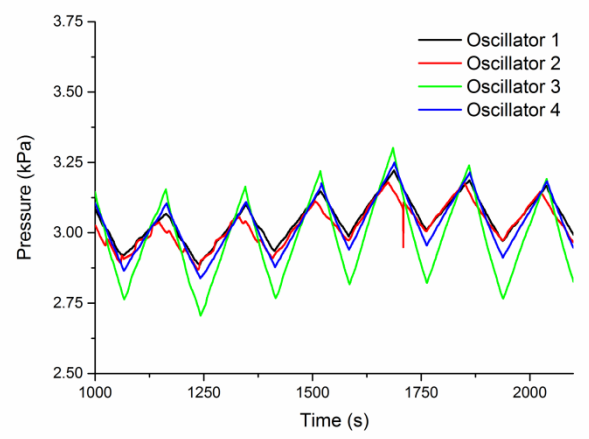|	a=c=2.6µL/min b=d=5µL/min	a=c=5µL/min b=d=2.6µL/min	a=d=2.6µL/min b=c=5µL/min
1.5 mm	0.004	0.050	0.036
2.0 mm	0.274*	0.045	0.033
2.2 mm	0.581*	0.077	0.033
2.5 mm	0.682*	0.062	0.030
3.0 mm	2.672*	0.085	0.029
Direct Connection	5.409*	10.462*	11.337*

*Synchronized
Non-synchronized

(b)

µ

Figure 5

(a)

(b)

(c)